

Instability of Flow In Magnetic Nozzle

Hunt Feng

University of Saskatchewan

June 27, 2023

Outline of Presentation

- 1 Introduction
- 2 Spectral Method
- 3 Singular Perturbation
- 4 Future Work
- 5 Appendix: Numerical Experiments

Outline of Presentation

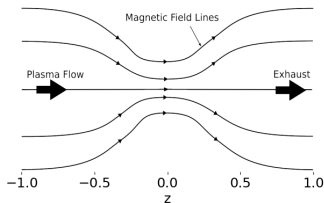
- 1 Introduction
- 2 Spectral Method
- 3 Singular Perturbation
- 4 Future Work
- 5 Appendix: Numerical Experiments

Linear Instability of Plasma Flow

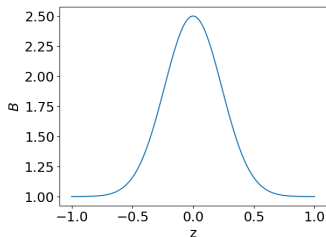
- The instability of plasma flow refers to the tendency of a plasma system to deviate from a stable, equilibrium state and exhibit perturbations or fluctuations in its behavior. [1]
- To investigate linear instability, we assume oscillating perturbed quantities, $\tilde{n}, \tilde{v} \sim \exp(-i\omega t)$.
 - ① If $\text{Im}(\omega) > 0$, then it is unstable flow since the perturbations grow exponential in time, $\exp(\text{Im}(\omega)t)$.
 - ② If $\text{Im}(\omega) \leq 0$, then it is stable flow since the perturbations decay/unchanged in time.
- In this research we will focus on the linear instability only.

Magnetic Nozzle

- A magnetic nozzle is a device that uses a magnetic field to shape and control the flow of charged particles in a plasma propulsion system.
- Instabilities may affect magnetic nozzle operation and the resulting thrust. [4]



(a) Simplified representation of magnetic nozzle.



(b) A simplified magnetic field of magnetic nozzle.

Figure 1: Simplified representation of magnetic nozzle. Length is normalized.

Governing Equations

The nondimensionalized governing equations for the plasma flow in magnetic nozzle are

$$\text{Cons. of Den.} \quad \frac{\partial n}{\partial t} + n \frac{\partial v}{\partial z} + v \frac{\partial n}{\partial z} - nv \frac{\partial_z B}{B} = 0 \quad (1)$$

$$\text{Cons. of Mom.} \quad n \frac{\partial v}{\partial t} + nv \frac{\partial v}{\partial z} = - \frac{\partial n}{\partial z} \quad (2)$$

where n, v are density and velocity, respectively.

The equilibrium quantities n_0, v_0 must satisfy the condition,

$$\frac{\partial}{\partial z} \left(\frac{n_0 v_0}{B} \right) = 0 \quad (3)$$

$$v_0 \frac{\partial v_0}{\partial z} = - \frac{1}{n_0} \frac{\partial n_0}{\partial z} \quad (4)$$

Equilibrium Velocity Profiles

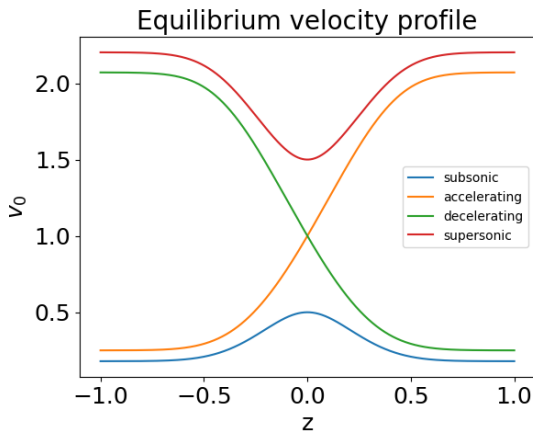


Figure 2: Velocity if normalized to sound speed. There are 4 different cases for velocity profile, subsonic, supersonic, accelerating and decelerating case.

Flow in Magnetic Mirror Configuration

- Magnetic nozzle has the magnetic mirror configuration.
- Bondi-Parker flow is a plasma flow in magnetic mirror configuration.
- Solar wind is an example of Bondi-Parker flow.
- It is interesting to study the instability of flow in such configuration.

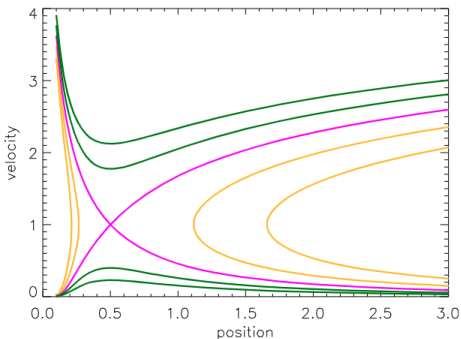


Figure 3: Equilibrium velocity profile of Bondi-Parker flow taken from [5].

Polynomial Eigenvalue Problem

By linearizing the governing equations, and assume oscillating perturbed quantities, $\tilde{n}, \tilde{v} \sim \exp(-i\omega t)$. We can derive the following equation,

$$\begin{aligned} & \omega^2 \tilde{v} \\ & + 2i\omega \left(v_0 \frac{\partial}{\partial z} + \frac{\partial v_0}{\partial z} \right) \tilde{v} \\ & + \left[(1 - v_0^2) \frac{\partial^2}{\partial z^2} - \left(3v_0 + \frac{1}{v_0} \right) \frac{\partial v_0}{\partial z} \frac{\partial}{\partial z} \right. \\ & \quad \left. - \left(1 - \frac{1}{v_0^2} \right) \left(\frac{\partial v_0}{\partial z} \right)^2 - \left(v_0 + \frac{1}{v_0} \right) \frac{\partial^2 v_0}{\partial z^2} \right] \tilde{v} = 0 \end{aligned} \tag{5}$$

It is a polynomial eigenvalue problem.

Outline of Presentation

- 1 Introduction
- 2 Spectral Method
- 3 Singular Perturbation
- 4 Future Work
- 5 Appendix: Numerical Experiments

Spectral Method

Eq.(5) can be reformulated as

$$\begin{bmatrix} 0 & 1 \\ \hat{M} & \hat{N} \end{bmatrix} \begin{bmatrix} \tilde{v} \\ \omega \tilde{v} \end{bmatrix} = \omega \begin{bmatrix} \tilde{v} \\ \omega \tilde{v} \end{bmatrix} \quad (6)$$

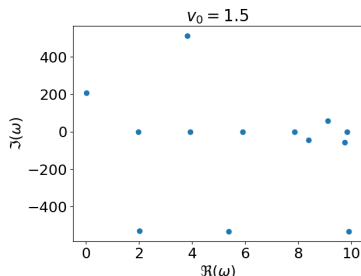
where the operators \hat{M} and \hat{N} are defined as

$$\begin{aligned} \hat{M} = & - \left[(1 - v_0^2) \frac{\partial^2}{\partial z^2} - \left(3v_0 + \frac{1}{v_0} \right) \frac{\partial v_0}{\partial z} \frac{\partial}{\partial z} \right. \\ & \left. - \left(1 - \frac{1}{v_0^2} \right) \left(\frac{\partial v_0}{\partial z} \right)^2 - \left(v_0 + \frac{1}{v_0} \right) \frac{\partial^2 v_0}{\partial z^2} \right] \\ \hat{N} = & -2i \left(v_0 \frac{\partial}{\partial z} + \frac{\partial v_0}{\partial z} \right) \end{aligned}$$

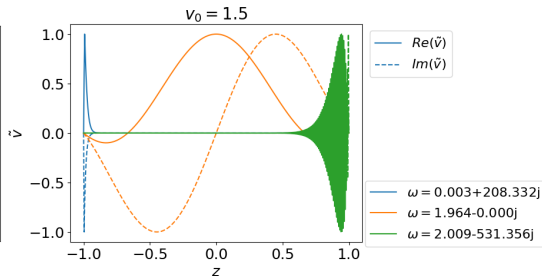
Then by discretizing operators \hat{M}, \hat{N} , this becomes an algebraic eigenvalue problem.

Spectral Pollution

- Analytical result shows all modes of Eq.(5) with $v_0 = \text{const}$ are stable.
- Finite-difference, finite-element, and spectral element discretization all show spurious unstable modes.



(a) Unfiltered eigenvalues.



(b) First few unfiltered eigenfunctions.

Figure 4: Finite difference discretization was used. Spurious modes occurs regardless of the resolution.

Convergence Test

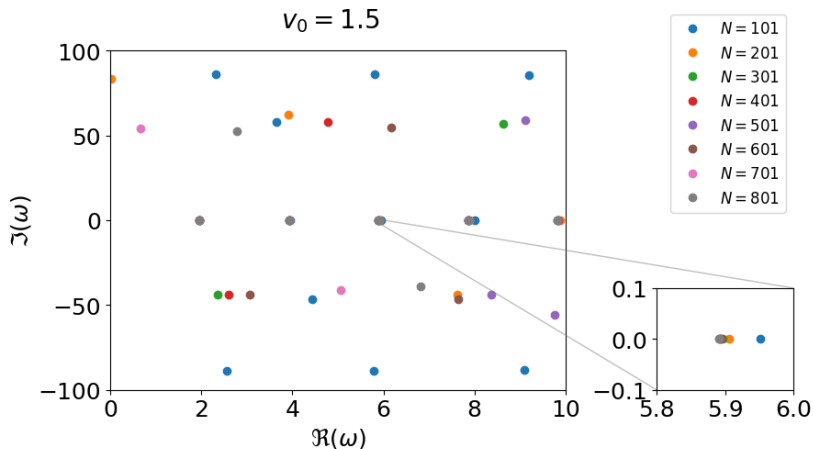
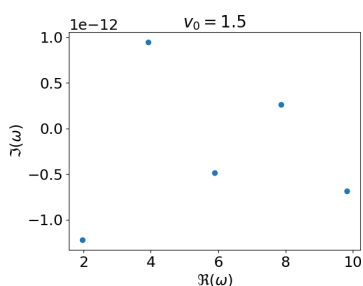
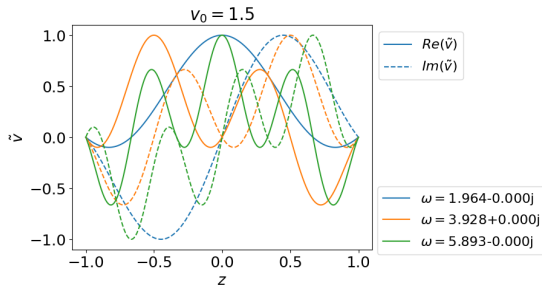


Figure 5: Pickup the convergent eigenvalues using convergence test.

Filtering Spurious Modes



(a) Filtered eigenvalues.



(b) First few filtered eigenfunctions.

Figure 6: The spurious modes are changing under different resolution. We can filter them by convergence test.

Outline of Presentation

- 1 Introduction
- 2 Spectral Method
- 3 Singular Perturbation**
- 4 Future Work
- 5 Appendix: Numerical Experiments

Existence of Singularity

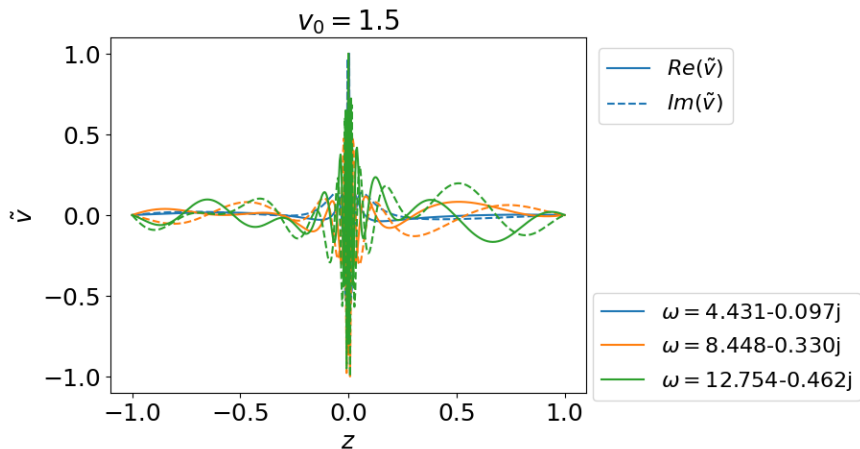


Figure 7: Dirichlet boundary conditions are set at the two ends, all eigenfunctions are squeezed to the singular point.

Interesting Connection to Black Hole

- The sonic horizon is an exact sonic analogue of black hole horizon. [6]
- A quasi-1D fluid flow is ruled by [2]

$$\frac{\partial}{\partial t}(\rho A) + \frac{\partial}{\partial x}(\rho A v) = 0 \quad (7)$$

$$\frac{\partial}{\partial t}(\rho A v) + \frac{\partial}{\partial x}[(\rho v^2 + p)A] = 0 \quad (8)$$

$$\frac{\partial}{\partial t} \left(\frac{\rho v^2}{2} - \frac{p}{1-\gamma} A \right) + \frac{\partial}{\partial x} \left[\left(\frac{\rho v^2}{2} - \frac{\gamma}{1-\gamma} A \right) A v \right] = 0 \quad (9)$$

In [2, 3], the acoustic analogue of tortoise coordinate is used to transform the above to Schrödinger-type equation,

$$x^* = c_{s0} \int [c_s(x)(1 - M(x)^2)]^{-1} dx$$

where c_{s0} denotes the stagnation speed of sound, $c_s = dp/d\rho$ is the local speed of sound and $M(x) = v(x)/c_s(x)$ is the Mach number.

Shooting Method

- Employed shooting method.
- Expanded \tilde{v} near singularity.
- Picked up regular solution.
- Shoot regular solution to the left and match boundary condition.

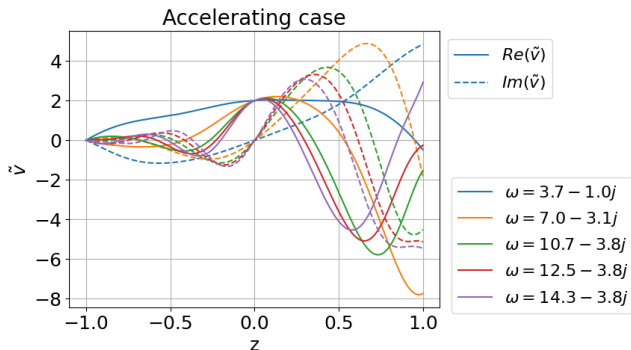


Figure 8: The solutions cross the singular point smoothly. All modes are stable.

Outline of Presentation

- 1 Introduction
- 2 Spectral Method
- 3 Singular Perturbation
- 4 Future Work**
- 5 Appendix: Numerical Experiments

Future Work

- Investigate and interpret the instability of an accelerating flow with non-zero left boundary. See Fig.9
- Compare results to analytically solvable problems with similar configuration.

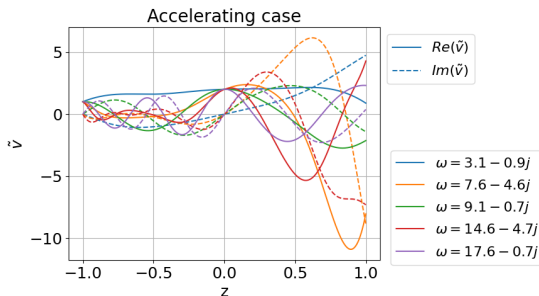


Figure 9: What is the physical interpretation of "non-zero" boundary value? How do we interpret these eigenvalues?



F. F. Chen.

Introduction to Plasma Physics and Controlled Fusion.
Springer International Publishing, Cham, 2016.



R. da Rocha.

Black hole acoustics in the minimal geometric deformation of a de Laval nozzle.

The European Physical Journal C, 77(5):355, 5 2017.
[Online; accessed 2023-03-02].



H. Furuhashi, Y. Nambu, and H. Saida.

Simulation of an acoustic black hole in a Laval nozzle.
Class. Quantum Grav., 23(17):5417–5438, Sept. 2006.



I. D. Kaganovich, A. Smolyakov, Y. Raitses, E. Ahedo, I. G. Mikellides, B. Jorns, F. Taccogna, R. Gueroult, S. Tsikata, A. Bourdon, J.-P. Boeuf, M. Keidar, A. T. Powis, M. Merino, M. Cappelli, K. Hara, J. A. Carlsson, N. J. Fisch, P. Chabert, I. Schweigert, T. Lafleur, K. Matyash, A. V. Khrabrov, R. W. Boswell, and A. Fruchtman.

Physics of $E \times B$ discharges relevant to plasma propulsion and similar technologies.

Physics of Plasmas, 27(12):120601, 12 2020.



E. Keto.

Stability and solution of the time-dependent Bondi–Parker flow.

Monthly Notices of the Royal Astronomical Society,
493(2):2834–2840, Apr. 2020.



W. Unruh.

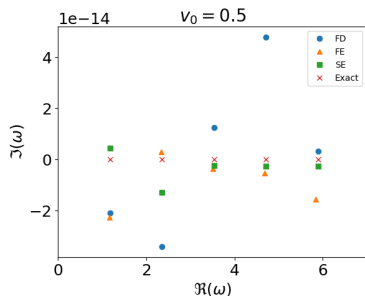
Sonic analogue of black holes and the effects of high frequencies on black hole evaporation.

Physical review. D, Particles and fields, 51(6):2827–2838, 1995.

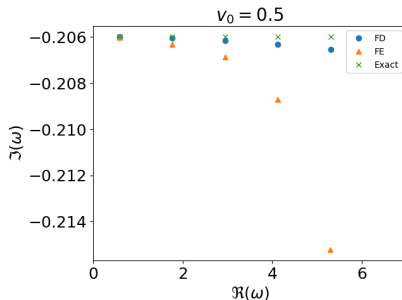
Outline of Presentation

- 1 Introduction
- 2 Spectral Method
- 3 Singular Perturbation
- 4 Future Work
- 5 Appendix: Numerical Experiments**

Constant Velocity Case - Subsonic



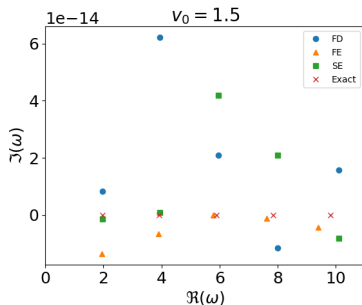
(a) Dirichlet boundary, all modes are stable.



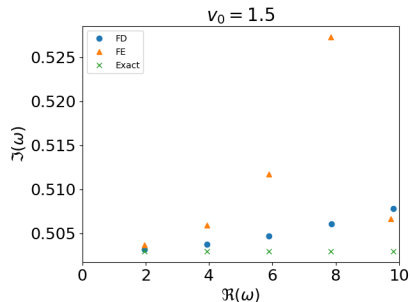
(b) Fixed-open boundary, all modes are stable.

Figure 10: Showing the first 5 eigenvalues. In the Dirichlet boundary case, all methods are close to the exact eigenvalues. Meanwhile, finite-difference method has higher accuracy than finite-element method in fixed-open case.

Constant Velocity Case - Supersonic



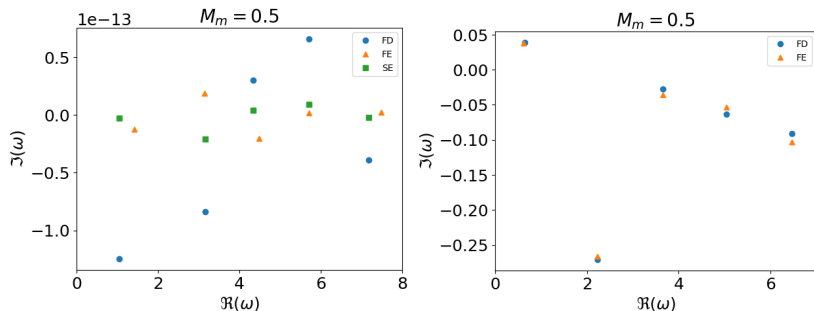
(a) Dirichlet boundary, filtered modes are stable.



(b) Fixed-open boundary, all modes are unstable.

Figure 11: Showing the first 5 eigenvalues. In the Dirichlet boundary case, all methods are close to the exact eigenvalues. Meanwhile, finite-difference method has higher accuracy than finite-element method in fixed-open case.

Subsonic Case

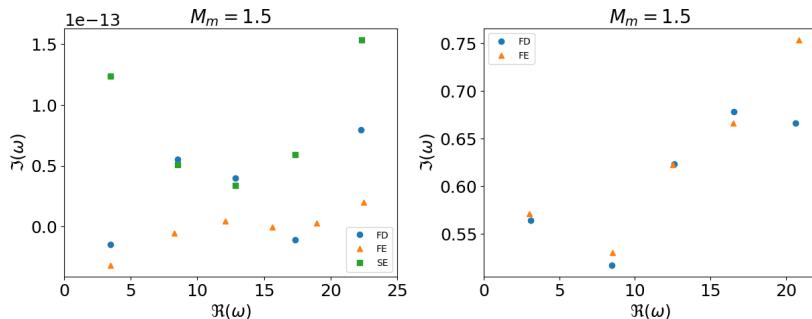


(a) Dirichlet boundary, all modes are stable.

(b) The ground mode is unstable, other modes are stable.

Figure 12: Showing the first 5 modes. It suggests that the subsonic flow in magnetic nozzle is stable.

Supersonic Case



(a) Dirichlet boundary, filtered modes are stable.

(b) Fixed-open boundary, all modes are unstable.

Figure 13: This suggests that the supersonic flow is stable if the boundary is Dirichlet and unstable if the boundary is left-fixed-right-open.

Accelerating Case

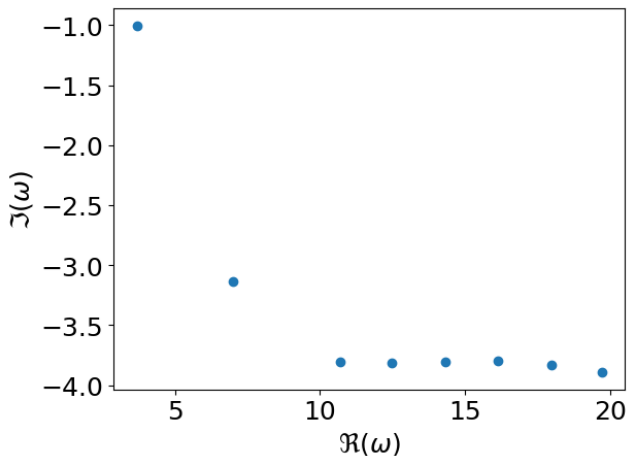


Figure 14: All modes are stable.